Journal of the Serbian Chemical Society
JSCS-info@shd.org.rs • www.shd.org.rs/JSCS
J. Serb. Chem. Soc. *85* (3) 335–346 (2020)
JSCS–5304
UDC 612.398:577.354:542.97+519.8:615.277
Original scientific paper

In silico studies on smoothened human receptor and its antagonists in search of anticancer effects

ANA BOROTA*, SORIN AVRAM, RAMONA CURPAN, ALINA BORA, DANIELA VARGA, LILIANA HALIP and LUMINITA CRISAN**

"Coriolan Dragulescu" Institute of Chemistry, Romanian Academy, 24 Mihai Viteazul Avenue, RO-300223, Timisoara, Romania

(Received 3 April, revised 5 July, accepted 6 August 2019)

Abstract: Lately, the cancers related with abnormal hedgehog (Hh) signalling pathway are targeted by smoothened (SMO) receptor inhibitors that are rapidly developing. Still, the problems of known inhibitors such as severe side effects, weak potency against solid tumors or even the acquired resistance need to be overcome by developing new suitable inhibitors. To explore the structural requirements of antagonists needed for SMO receptor inhibition, pharmacophore mapping, 3D-QSAR models, database screening and docking studies were performed. The best selected pharmacophore hypothesis based on which statistically significant atom-based 3D-QSAR model was developed (R^2 = = 0.856, Q^2 = 0.611 and Pearson-R = 0.817), was further subjected to dataset screening in order to evaluate its ability to prioritize active compounds over decoys. The efficiency of one four-points pharmacophore hypothesis (AAHR.524) was observed based on good evaluation metrics such as the area under the curve (0.795), and weighted average precision (0.835), suggesting that the model is trustworthy in predicting novel inhibitors against SMO receptor.

Keywords: pharmacophore; 3D-QSAR; docking; SMO inhibitors.

INTRODUCTION

The smoothened (SMO) receptor is a G-protein-coupled receptor (GPCR)--like protein and it is one of the relevant components of the hedgehog (Hh) signalling pathway[1]. GPCR are seven transmembrane receptors which constitute the largest family of human proteins[2] that regulate a various multitude of intracellular signalling cascades.[3] Late breakthroughs in GPCRs biochemistry[4,5] have enhanced our knowledge of drug action on these significant targets, which will lead to the design of better therapeutics in the future.

*,** Corresponding authors. E-mail: (*)ana_borota@acad-icht.tm.edu.ro; (**)lumi_crisan@acad-icht.tm.edu.ro
https://doi.org/10.2298/JSC190403085B

It is known that ~25 % of cancers present aberrant Hh pathway activation.[6] Regarding the implication of Hh pathway in cancer, three models of action have been proposed.[7] The first type is ligand independent and refers to mutations in Hh pathway components, that have been associated with medulloblastoma and basal cell carcinomas.[8,9] The II (autocrine) and III (paracrine) types of mechanisms are ligand dependent and include: lung,[10] pancreatic,[11] colorectal,[12] breast,[13] gastrointestinal tract,[14] prostate,[15] glioma tumours[9] and hematological malignancies.[16] The growth of these types of tumours can be suppressed by different pathway inhibitors, such as SMO receptor antagonists.[17] Indeed, a number of SMO antagonists (such as: CUR61414, IPI-926, BMS-833923, PF-04449913, LEQ-506 and TAK-441) have demonstrated anticancer activity and have entered the clinical trials. Hitherto, FDA approved two SMO antagonists (LDE225/ /Sonidegib and GDC-0449/Vismodegib) for the treatment of basal cell carcinoma.[18] Unfortunately, these two inhibitors have shown severe side effects, along with weak potency against solid tumours, and, moreover, an issue related to acquired resistance has been identified.[1,19] To overcome these downsides, many studies have focused on designing new and diverse SMO inhibitors, with desirable selectivity against the target of interest.[20] In this regard, a recently synthetized and biologically evaluated series of 26 compounds[21] as SMO antagonists (Table I) was used for computational investigation.

Ligand- and structure-based approaches were involved in order to understand which are the essential features responsible for the inhibition of SMO receptor. Phase software (Schrödinger)[22] was used for the generation of ligand-based pharmacophore models and 3D-QSAR module was employed to validate the models. An external validation of the best pharmacophore hypothesis was achieved based on virtual screening (VS) and statistical evaluation of the results. The importance of stereochemical aspects involved in ligand-receptor interactions were highlighted based on the rigid and flexible docking studies performed with Glide[23] and Induced Fit[24] programs.

COMPUTATIONAL METHODS

Pharmacophore generation protocol

In the current study, a dataset of 26 compounds newly synthesized and biologically tested against SMO receptor, by Lu and collaborators[21] (Table S-I of the Supplementary material to this paper) was the subject of computational analysis for pharmacophore generation and docking studies. The preparation of the ligands for *in silico* studies along with the steps followed for the generation of pharmacophore hypotheses are presented in detailed manner in the Supplementary material.

Phase[22] with the option: "Develop Common Pharmacophore Hypotheses" was used for the generation and validation of the pharmacophore hypotheses by the involvement of the atom-based QSAR module. The following features: hydrogen bond donor/acceptor, hydrophobic, negative, positive and aromatic rings were taken in account for the generation of the pharmacophore hypotheses. In order to select the best hypothesis, an atom-based 3D-QSAR

analysis was carried out using three partial least-squares (PLS) factors. The test set compounds that represent roughly 23 % of the dataset were selected to cover the same range of activity as the compounds from the training set.[25] The multidimensional descriptor space between the training and test set was checked[26] using 2D fingerprints. The well-known 2D Tanimoto and Euclidean distance coefficients, and the median values for important 2D properties of molecules were calculated (Supplementary material).

The best selected pharmacophore hypothesis was employed in VS experiments using the "Advanced Pharmacophore Screening" option of Phase software (the inter-site distance matching tolerance was of 2Å for minimum four site points) to test its ability to distinguish active compounds or positives from inactive ones or negatives (assumed to be the decoys). For this purpose, an external validation dataset was assembled, and it was realized following the protocol described in the Supplementary material.

The VS results were evaluated using an in-house developed program, "Evaluation" tool In ChemInformatics (ETICI 1.6).[27] The following statistical metrics (Eqs. (1)–(5)) were used for the evaluation: receiver operating characteristics (ROC) curve and its corresponding area under the curve (*AUC*)[28] Boltzmann enhanced discrimination of ROC (BEDROC)[29], precision (*PPV*)[30], accuracy (*Acc*), sensitivity (*Se*), specificity (*Sp*)[31] and the true positive (*TP*) at 1, 2, 5, 10 % of false positives (*FP*s):[32]

$$AUC = 1 - \frac{1}{TP + FN} \sum_{i=1}^{TP+FN} FPR_i \tag{1}$$

$$PPV = \frac{TP}{TP + FP} \tag{2}$$

$$Se = \frac{TP}{TP + FN} \tag{3}$$

$$Sp = \frac{TN}{TN + FN} \tag{4}$$

$$Acc = \frac{TP + TN}{TP + TN + FP + FN} \tag{5}$$

where: *TP* indicates the correctly predicted actives; *FN* designates the incorrectly identified inactives; *FPR* is false positive rate*; TN* represents the correctly predicted inactives or negatives and *FP* denotes the incorrectly predicted actives or positives.

AUC parameter is used to evaluate the models performance in classification, to discriminate actives from inactives and it takes values in the range 0 to 1. The closer *AUC* value is to 1 the better a model discerns true positive from false positive results.[28] BEDROC can be considered as a "virtual screening usefulness scale" while ROC assesses "improvement over random scale". The difference between the two aforementioned evaluation parameters is that ROC relates to a uniform distribution and BEDROC refers to an exponential distribution.[29] For imbalance class when the number of actives is lower than a number of inactives, the precision parameter was replaced with weighted average precision.[33]

Docking simulations protocol

The best resolution X-ray structure of SMO receptor was extracted from PDB (PDB ID: 4jkv) and prepared for docking studies with the "Protein Preparation Wizard" module from Schrödinger suite. Briefly, the following steps were employed: the bond orders were assigned; the Chemical Components Dictionary (CCD) database was used; hydrogens were added;

create zero-order bonds to metals parameter was selected; disulfide bonds were created; waters beyond 5 Å were deleted and missing side-chains were added to the protein. The proper ionization state of the co-crystallized ligand (LY2940680), at physiological pH of 7.0–7.4 was generated and the H-bond assignment was performed using PROPKA module, setting pH to 7.0. Finally, the protein was energetically minimized with OPLS_2005 force field until an RMSD of 0.3 Å for heavy atoms was reached.

A molecular docking study was carried out with "Glide"[23] and "Induced Fit"[24] protocol included in Schrödinger suite. "Glide" module[23] was used in standard precision (S*P*) mode with default settings, *i.e.*, scaling factor of 0.8, partial charge cut-off of 0.15 and only the flexibility of ligands was considered. "Induced Fit" docking protocol[24] accounts also for protein flexibility and it was carried out with the following settings: *SP* option, receptor and ligand van der Waals scaling of 0.50.

RESULTS AND DISCUSSION

Analysing the results generated by Phase,[22] 22 categories of four features common pharmacophore hypotheses (CPH) were identified. CPH include the same features placed together in similar spatial arrangements. All hypotheses received a good survival score (values > 3) and were subjected to QSAR model development. A QSAR model is reliable if a number of statistical parameters meet certain condition as follows: R^2 (squared correlation coefficients for the training set) > 0.6; Q^2 (squared correlation coefficients for the test set) > 0.5;[26] Pearson-R (correlation between the predicted and observed activity for the test set) > 0.5; p (the significance level of variance ratio) < 0.05; *SD* (standard deviation) and *RMSE* (root mean square error) should have low values, while F (variance ratio) should have high value.[22,34] The best hypothesis named AAHR.524 with a survival score of 5.263 has statistical significant results (Table I).

TABLE I. The statistical parameters for the AAHR.524 hypothesis obtained

PLS factor	*SD*	R^2	p	F	*RMSE*	Q^2	Pearson-R
1	0.255	0.601	6.00E-05	27.100	0.308	0.470	0.760
2	0.195	0.779	2.72E-06	29.900	0.303	0.486	0.769
3	0.161	0.859	4.90E-07	32.500	0.263	0.611	0.817

For AAHR.524 hypothesis the distances between pharmacophore sites are shown in Fig. 1 and scatter plots of experimental versus predicted bioactivity values for training and test set are presented in Fig. 2.

In order to highlight favorable and unfavorable regions for ligand–protein interactions, the atom-based 3D-QSAR model regarding hydrogen bond donor, hydrophobic and electron withdrawing properties was mapped against the pharmacophore model (Fig. 3). Additionally, the AAHR.524 hypothesis was validated in virtual screening (VS) experiments using Phase Advanced Pharmacophore Screening (Fig. 4). In Fig. 3 the combined effects for all the features retrieved in the workspace ligands along with the overlapping of the best fitted and the less active ligands are depicted. The favorable regions for biological activity

are represented by blue cubes, while the red cubes indicate detrimental regions. For the AAHR.524 hypothesis, the presence of blue cubes in the region of the –NH– group of compound **17** (Fig. 3b) indicates that hydrogen bond donor property of this group is favorable for activity. This finding is also supported by Glide docking results which highlight the contribution of this amino group in the formation of a hydrogen bond with residue Tyr 394 of the SMO binding site.

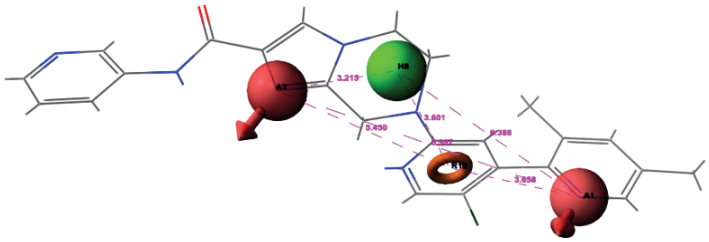

Fig. 1. AAHR.524 pharmacophore hypothesis depicted with the best fitted compound **17**. The distances between the following features are presented: hydrogen bond acceptor (A1), hydrogen bond acceptor (A3), aromatic ring (R12) and one hydrophobic region (H8).

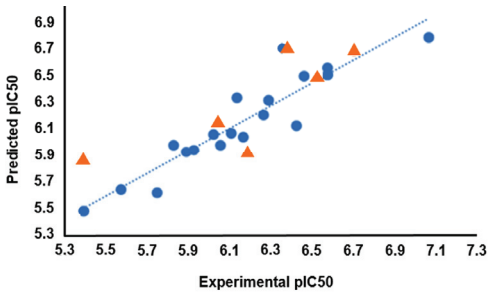

Fig. 2. Correlation plots of the experimental versus Phase predicted activity of training set (circles) and test set (triangles) for AAHR.524 hypothesis.

The pyridine ring of compound **17** is engaged in hydrophobic interactions with the binding site, while in the less active ligand (compound **22**) this feature is missing (Fig. 3c). This finding was also confirmed by docking studies. Regarding the electron withdrawing property (Fig. 3a), the Glide docking study revealed that the oxygen atom of the carbonyl group of compound **17** can act as hydrogen bond acceptor for Arg400 residue.

In order to assess the efficiency of VS experiments, it is necessary to test their ability to distinguish active compounds or positives from inactive ones or negatives (assumed to be the decoys). In this regard, different evaluation operators were employed. Namely, the receiver operation characteristics (ROC) curve[28] (Fig. 4) was used for the visualization of the true positive rate (*TPR*) *versus* the false positive rate (*FPR*) and the area under the curve (*AUC*) was calculated. In our experiment, a good scores for: *AUC* of 0.795 (±0.027), *Se* (the

fraction of actives correctly predicted) of 0.587, *Sp* (the fraction of inactives correctly predicted) of 0.647, *Acc* (the fraction of correct predictions) of 0.640, *WPPV* (weighted average precision) of 0.835 and BEDROC (α = 20) of 0.766, were obtained, suggesting that the AAHR.524 pharmacophore hypothesis provides a good class separation. Additionally, good enrichment factors, *TP* at x of *FP*s were obtained: 19.047 % at x = 1 %; 30.476 % at x = 2 %; 42.857 % at x = 5 %; 56.190% at x = 10 %.

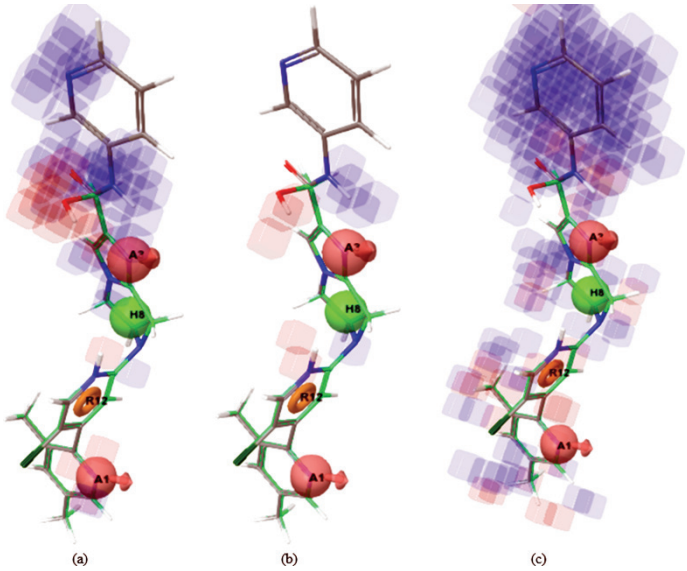

Fig. 3. Superposition of compound **17** (best fitted over AAHR.524 hypothesis) represented by grey carbon atoms with compound **22** (least active ligand) depicted by green carbon atoms: a) electron withdrawing property; b) hydrogen bond donor property; c) hydrophobic property.

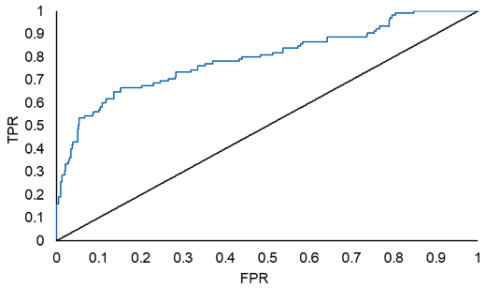

Fig. 4. The receiver operation characteristics (ROC) curve, involving the AAHR.524 hypothesis against the validation data set.

In Fig. 4 is depicted the ROC curve, the diagonal represents the random sampling of compounds (actives and decoys) and it separates two classification areas: the correctly predicted compounds are shown above, while the incorrectly

classified compounds occupy the underneath area. *TPR* represents the fraction of correctly classified positives (actives) from the total of positives, while *FPR* expresses the fraction of the incorrectly classified negatives (decoys) from the total negatives.[28,35] Following ligand-based analysis, the structure-based study, represented by molecular docking, bring additional light on ligand-protein interaction profile.

In order to validate the reasonability of choosing the two docking software for our study (Glide (Fig. 5a) and Induced Fit (Fig. 5b)), we have undertaken a control experiment. The co-crystallized inhibitor LY2940680 was docked to its native X-ray structure, 4jkv, and the best docked pose was superimposed with the native binding pose from the experimental structure 4jkv.

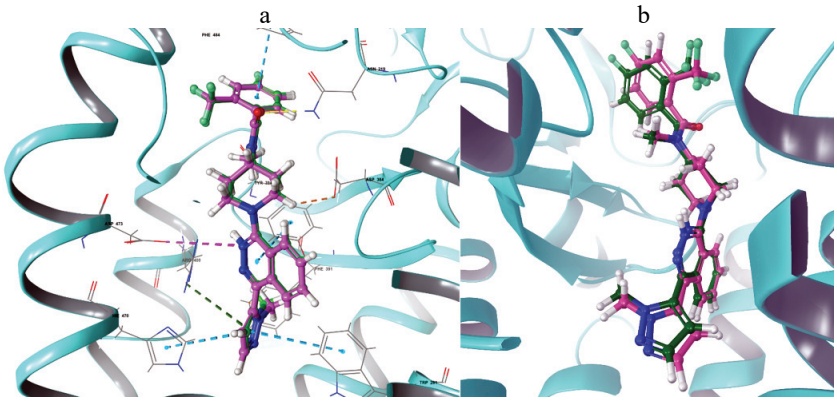

Fig. 5. Superposition of the pose of the crystal structure 4jkv (with the inhibitor LY2940680), and the pose of the same ligand obtained by docking with Glide SP (a) superposition of the pose of the crystal structure 4jkv (with the inhibitor LY2940680), and the pose of the same ligand obtained by docking with Induced Fit SP (b).

The *RMSD* values were also calculated. According to Gohlke *et al.*,[35] an *RMSD* value less than 2.0 Å is broadly accepted as "effectively" docked structure. The docking protocol with Glide and Induced Fit have provided very good *RMSD* values of 0.192 (Fig. 5a), and 0.700, respectively (Fig. 5b).

A comparative study made by Wang *et al.*[36] on the binding profile and interactions of the ligands: antagonists and agonists at the human SMO receptor, reveals some specific features. The binding sites of antagonists, *e.g.*, LY2940680, cyclopamine and AntaXV and the agonist SAG1.5 consist mostly of residues from the extracellular linker domain and loops. In particular, Asp219 (of the extracellular linker domain) it involved in the formation of hydrogen bonds with ligands: LY2940680, AntaXV and SAG1.5.[36] Also, an important residue from the helix V is Arg400 (Arg5.39) which forms hydrogen bonds with antagonists: LY2940680 and AntaXV.[36,37] According to the latest studies, the SMO receptor

contains two distinct binding sites. One ligand-binding site is located in heptahelical transmembrane domain, and the second, occupied by a cholesterol molecule, is placed in the extracellular cysteine-rich domain.[38] Thus, the SMO inhibitors were classified in two categories: 1) antagonists that bind mainly to the extracellular loops and 2) antagonists that enter deeper into the cavity formed by the transmembrane helices domain.[20]

The large binding site of SMO receptor allows flexibility to the ligands leading to several distinct binding modes.[20,36–38] Although, similar disposition of the ligand *in situ* were retrieved by the two docking methods employed (Fig. 6c), the orientation of the ligand is reversed in the binding site, hence resulting in different interactions with the amino acids of the protein (Fig. 6a and b). Two interaction patterns for compound **17** were observed depending on the docking software used, Glide (Fig. 6a) or Induced Fit (Fig. 6b).

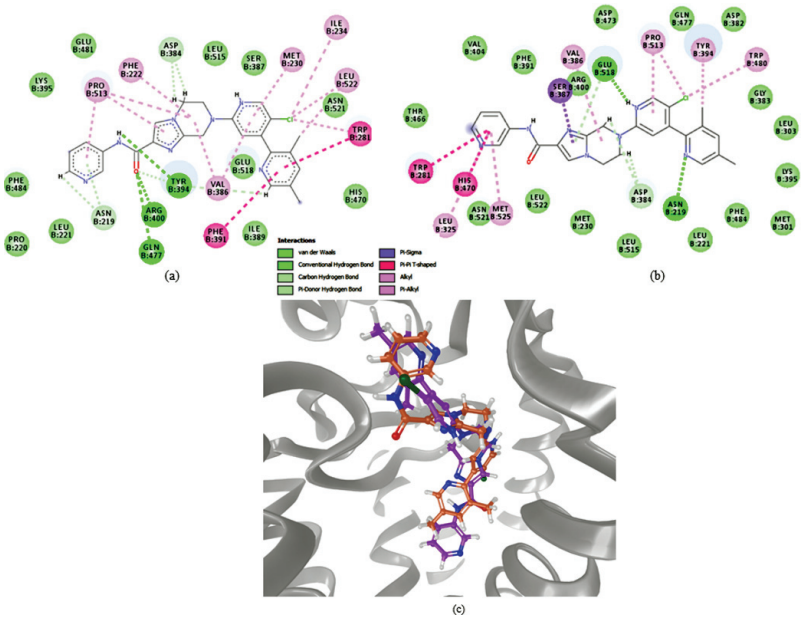

Fig. 6. Representation of the interactions map of the best docked pose of compound **17** with the amino acids of SMO human binding site: glide docking (a); induced fit docking (b); their superposition in situs (c).

Following the most important features characterizing the interaction of compound **17** with the binding site of SMO receptor resulted from docking with Glide are presented: *i*) the oxygen atom of the carbonyl group acts like hydrogen bond acceptor for Arg400 and Gln 477; *ii*) the aliphatic –NH– group is hydrogen bond donor to Tyr394; *iii*) the dimethyl-pyridine ring is involved in π–π stacking

interactions with Trp281 and Phe391; *iv*) the chlorine atom is involved in alkyl interactions with Ile234, Leu522 and Trp281 (Fig. 6a).

The following main interactions were found when the compound was docked with Induced Fit protocol: *i*) the N= atom of dimethylpyridine is acting as hydrogen bond acceptor for Asn219; *ii*) the –NH= group of chloropyridine is functioning as hydrogen bond donor to Glu518; and *iii*) the pyridine ring is involved in π–π stacking interactions with Trp281 and His470 residues (Fig. 6b).

Also, the ligand rings are involved in multiple hydrophobic interactions with residues of the binding site, *e.g.*, Pro513, Trp281, Val386, Leu325, Met525, His470 and Ser387 (Fig. 6a and b), leading to the stabilization of the ligand into the binding pocket.

The amino acids Arg400 and Tyr394 which interact with compound **17**, are also known to be important for the interaction with other SMO antagonists. The relevance of these two amino acids in the antagonistic binding is supported by crystallographic studies.[36–38]

It can be seen from the Fig. 6b that three pharmacophore features of the four of AAHR.524 hypothesis are recapitulated in the best docking pose resulted from Induced Fit, only the interaction with the acceptor (A3) is missing.

CONCLUSIONS

In order to discover the common features of inhibitors of SMO receptor with potential anticancer benefits, ligand-based pharmacophore models were first generated. The best pharmacophore hypothesis turned out to be AAHR.524, with the following characteristics: two hydrogen bond acceptors (A), one hydrophobic (H) site and one aromatic ring (R). The pharmacophore hypothesis was found to be statistically significant with the correlation coefficient, R^2 of 0.859 for the training set and the correlation coefficient, Q^2 of 0.611 for the test set. Virtual screening experiments and molecular docking were involved in the evaluation of the models and to gain insights into the ligand-receptor interaction profile. Considering the large size of the binding site, as well as the different binding patterns of inhibitors to the site, our pharmacophore model being built on a congeneric series of inhibitors it is assumed to lead to increased specificity and reduced diversity in virtual screening experiments. However, we can say that the pharmacophore model was validated through a virtual screening experiment with reliable values of the evaluation metrics, *e.g.*, *AUC* of 0.795, and enrichment factors. In addition, it can be seen that our docking results reproduce the main interactions with key residues (*e.g.*, Asn219, Arg400, Tyr394 and Asp384) found in the X-ray crystal structure (PDB ID: 4jkv). Between the two docking approaches used: Glide and Induced Fit, the last one which accounts also for protein flexibility has led to better results. The validated pharmacophore model obtained suggests that it could

be reliably used in predicting novel, promising inhibitors against SMO receptor with potential anticancer activity.

SUPPLEMENTARY MATERIAL

Additional data are available electronically from http://www.shd.org.rs/JSCS/, or from the corresponding author on request.

Acknowledgements. This project was financially supported by Project 1.1 of the "Coriolan Dragulescu" Institute of Chemistry, Romanian Academy. The authors thank to the Chemaxon Ltd. and OpenEye Ltd. for providing an academic license.

ИЗВОД

IN SILICO СТУДИЈЕ НА ЗАГЛАЂЕНОМ (*SMOOTHENED*) ХУМАНОМ РЕЦЕПТОРУ И ЊЕГОВИМ АНТАГОНИСТИМА У ПОТРАЗИ ЗА АНТИТУМОРСКИМ ЕФЕКТИМА

ANA BOROTA, SORIN AVRAM, RAMONA CURPAN, ALINA BORA, DANIELA VARGA, LILIANA HALIP и LUMINITA CRISAN

"Coriolan Dragulescu" Institute of Chemistry, Romanian Academy, 24 Mihai Viteazul Avenue, RO-300223, Timisoara, Romania

У новије време, канцери повезани са ненормалним хеџхог (Hh) сигналним путем (*hedgehog (Hh) pathway signalling*) се испитују преко инхибиторима заглађених рецептора (SMO, *Smoothened (SMO) receptor inhibitors*) који се брзо развијају. Међутим, проблеми са познатим инибиторима попут озбиљних споредних ефеката, слабе моћи против солидних тумора или чак стечене отпорности тек треба да се превазиђу развојем нових погодних инхибитора. Да би истражили структурне захтеве за антагонисте потребне за инхибицију SMO рецептора урадили смо: мапирање фармакофоре, 3D-QSAR моделе, претраживање база података и студије докинга. Најбоља хипотеза за фармакофору је одабрана, на основу ње је развијен статистички значајан атомски 3D-QSAR модел (R^2 = 0,856, Q^2 = = 0,611 и Pearson-R = 0,817), који је даље подвргнут скринингу, база података, како бу се проценила његова способност да издвоји активна једињења од лажно позитивних. Запажена је ефикасност четвороparаметарске (*four-points*) хипотезе фармакофоре (AAHR.524) на бази добре метрике процена попут површине испод криве (0,795) и прецизности одмереног просека (0,835) што сугерише да је модел поуздан за предвиђање нових инхибитора за SMO рецептор.

(Примљено 3. априла, ревидирано 5. јула, прихваћено 6. августа 2019)

REFERENCES

1. M. Ruat, L. Hoch, in *The Smoothened Receptor in Cancer and Regenerative Medicine*, M. Ruat, Ed., Springer, Berlin, 2015, pp. 1–11 (ISBN 978-3-319-19755-5)
2. G. Liapakis, A. Cordomí, L. Pardo, *Curr. Pharm. Des.* **18** (2012) 175 (http://dx.doi.org/10.2174/138161212799040529)
3. D. Hilger, M. Masureel, B. K. Kobilka, *Nat. Struct. Mol. Biol.* **25** (2018) 4 (http://dx.doi.org/10.1038/s41594-017-0011-7)
4. J. Shonberg, R. C. Kling, P. Gmeiner, S. Löber, *Bioorg. Med. Chem.* **23** (2015) 3880 (http://dx.doi.org/10.1016/j.bmc.2014.12.034)
5. L. Halip, A. Borota, M. Mracec, R. Curpan, A. Gruia, M. Mracec, *Rev. Roum. Chim.* **54** (2009) 157 (http://revroum.lew.ro/wp-content/uploads/2009/RRCh_2_2009/Art%2007.pdf)
6. K. K. Chahal, M. Parle, R. Abagyn, *Anti-Cancer Drugs* **29** (2018) 387 (http://dx.doi.org/10.1097/CAD.0000000000000609)

7. L. L. Rubin, F. J. de Sauvage, *Nat. Rev. Drug Discov.* **5** (2006) 1026 (http://dx.doi.org/10.1038/nrd2086)
8. C. Wicking, I. Smyth, A. Bale, *Oncogene* **18** (1999) 7844 (http://dx.doi.org/10.1038/sj.onc.1203282)
9. S. J. Scales, F. J. de Sauvage, *Trends Pharmacol. Sci.* **30** (2009) 303 (http://dx.doi.org/10.1016/j.tips.2009.03.007)
10. D. N. Watkins, D. M. Berman, S. G. Burkholder, B. Wang, P. A. Beachy, S. B. Baylin, *Nature* **422** (2003) 313 (http://dx.doi.org/10.1038/nature01493)
11. S. P. Thayer, M. P. di Magliano, P. W. Heiser, C. M. Nielsen, D. J. Roberts, G. Y. Lauwers, Y. P. Qi, S. Gysin, C. Fernández-del Castillo, V. Yajnik, B. Antoniu, M. McMahon, A. L. Warshaw, M. Hebrok, *Nature* **425** (2003) 851 (http://dx.doi.org/10.1038/nature02009)
12. D. Qualtrough, A. Buda, W. Gaffield, A. C. Williams, C. Paraskeva, *Int. J. Cancer* **110** (2004) 831 (http://dx.doi.org/10.1002/ijc.20227)
13. S. Mukherjee, N. Frolova, A. Sadlonova, Z. Novak, A. Steg, G. P. Page, D. R. Welch, S. M. Lobo-Ruppert, J. M. Ruppert, M. R. Johnson, A. R. Frost, *Cancer Biol. Ther.* **5** (2006) 674 (https://doi.org/10.4161/cbt.5.6.2906)
14. D. M. Berman, S. S. Karhadkar, A. Maitra, R. Montes de Oca, M. R. Gerstenblith, K. Briggs, A. R. Parker, Y. Shimada, J. R. Eshleman, D. N. Watkins, P. A. Beachy, *Nature* **425** (2003) 846 (http://dx.doi.org/10.1038/nature01972)
15. S. S. Karhadkar, G. S. Bova, N. Abdallah, S. Dhara, D. Gardner, A. Maitra, J. T. Isaacs, D. M. Berman, P. A. Beachy, *Nature* **431** (2004) 707 (http://dx.doi.org/10.1038/nature02962)
16. P. Lin, Y. He, G. Chen, H. Ma, J. Zheng, Z. Zhang, B. Cao, H. Zhang, X. Zhang, X. Mao, *Anti-Cancer Drugs* **29** (2018) 995 (http://dx.doi.org/10.1097/CAD.0000000000000679)
17. J. Jiang, C. C. Hui, *Dev. Cell.* **15** (2008) 801 (http://dx.doi.org/10.1016/j.devcel.2008.11.010)
18. T. K. Rimkus, R. L. Carpenter, S. Qasem, M. Chan, H. W. Lo, *Cancers* **8** (2016) 22 (http://dx.doi.org/10.3390/cancers8020022)
19. S. V. Mohan, A. L. Chang, *Clin. Cancer Res.* **21** (2015) 2677 (http://dx.doi.org/10.1158/1078-0432.CCR-14-3180)
20. M. Xin, X. Ji, L. K. de la Cruz, S. Thareja, B. Wang, *Med. Res. Rev.* **38** (2018) 870 (http://dx.doi.org/10.1002/med.21482)
21. W. Lu, D. Geng, Z. Sun, Z. Yang, H. Ma, J. Zheng, X. Zhang, *Bioorg. Med. Chem. Lett.* **24** (2014) 2300 (https://doi.org/10.1016/j.bmcl.2014.03.079)
22. S. L. Dixon, A. M. Smondyrev, E. H. Knoll, S. N. Rao, D. E. Shaw, R. A. Friesner, *J. Comput.-Aided Mol. Design* **20** (2006) 647 (http://dx.doi.org/10.1007/s10822-006-9087-6)
23. R. A. Friesner, J. L. Banks, R. B. Murphy, T. A. Halgren, J. J. Klicic, D. T. Mainz, M. P. Repasky, E. H. Knoll, D. E. Shaw, M. Shelley, J. K. Perry, P. Francis, P. S. Shenkin, *J. Med. Chem.* **47** (2004) 1739 (https://doi.org/10.1021/jm0306430)
24. W. Sherman, T. Day, M. P. Jacobson, R. A. Friesner, R. Farid, *J. Med. Chem.* **49** (2006) 534 (https://doi.org/10.1021/jm050540c)
25. A. Golbraikh, A. Tropsha, *J. Mol. Graph. Model.* **20** (2002) 269 (https://doi.org/10.1016/S1093-3263(01)00123-1)
26. A. Golbraikh, A. Tropsha, *J. Comput.-Aided Mol. Des.* **16** (2002) 357 (https://doi.org/10.1023/A:1020869118689)
27. S. I. Avram, L. M. Pacureanu, A. Bora, L. Crisan, S. Avram, L. Kurunczi, *J. Chem. Inform. Model.* **54** (2014) 2360 (http://dx.doi.org/10.1021/ci5002668)

28. J. A. Hanley, B. J. McNeil, *Radiology* **143** (1982) 29 (http://dx.doi.org/10.1148/radiology.143.1.7063747)
29. J. F. Truchon, C. I. J. Bayly, *J. Chem. Inform. Model.* **47** (2007) 488 (http://dx.doi.org/10.1021/ci600426e)
30. M. Hall, E. Frank, G. Holmes, B. Pfahringer, P. Reutemann, I. H. Witten, *SIGKDD Explor. Newsletter* **11** (2009) 10 (http://dx.doi.org/10.1145/1656274.1656278)
31. T. Fawcett, *Pattern Recog. Lett.* **27** (2006) 861 (http://dx.doi.org/10.1016/j.patrec.2005.10.010)
32. A. N. Jain, *J. Comput.-Aided Mol. Des.* **22** (2008) 201 (http://dx.doi.org/10.1007/s10822-007-9151-x)
33. E. Kotsampasakou, G. F. Ecker, *J. Chem. Inform. Model.* **57** (2017) 608 (http://dx.doi.org/10.1021/acs.jcim.6b00518)
34. B. Badhani, R. Kakkar, *J. Biomol. Struct. Dyn.* **35** (2017)1950 (http://dx.doi.org/10.1080/07391102.2016.1202863)
35. H. Gohlke, M. Hendlich, G. Klebe, *J. Mol. Biol.* **295** (2000) 337 (http://dx.doi.org/10.1006/jmbi.1999.3371)
36. C. Wang, H. Wu, T. Evron, E. Vardy, G. W. Han, X. P. Huang, S. J. Hufeisen, T. J. Mangano, D. J. Urban, V. Katritch, V. Cherezov, M. G. Caron, B. L. Roth, R. C. Stevens, *Nature Commun.* **10** (2014) 4355 (http://dx.doi.org/10.1038/ncomms5355)
37. C. Wang, H. Wu, V. Katritch, G. W. Han, X. P. Huang, W. Liu, F. Y. Siu, B. L. Roth, V. Cherezov, R. C. Stevens, *Nature* **497** (2013) 338 http://dx.doi.org/10.1038/nature12167)
38. E. F. X. Byrne, R. Sircar, P. S. Miller, G. Hedger, G. Luchetti, S. Nachtergaele, M. D. Tully, L. Mydock-McGrane, D. F. Covey, R. P. Rambo, M. S. P. Sansom, S. Newstead, R. Rohatgi, C. Siebold, *Nature* **535** (2016) 517 (http://dx.doi.org/10.1038/nature18934).